

# Feature Extraction from Laser Scan Data based on Curvature Estimation for Mobile Robotics

Pedro Núñez, Ricardo Vázquez-Martín, José C. del Toro, Antonio Bandera and Francisco Sandoval

Grupo de Ingeniería y Sistemas Integrados. Dpto. Tecnología Electrónica.

Universidad de Malaga, Campus de Teatinos 29071-Malaga (Spain)

Email: pmnt@uma.es

**Abstract**—This paper presents a geometrical feature detection system to use with conventional 2D laser rangefinders. This system consists of three main modules: data acquisition and pre-processing, rupture and breakpoint detection and feature extraction. The novelty of this system is a new efficient approach for natural feature extraction based on curvature estimation. This approach permits to extract and characterise line segments, corners and curve segments from the laser scan. Experimental results show that the proposed approach is very fast and permit to verify its effectiveness in indoor and outdoor environments.

## I. INTRODUCTION

Localisation is a fundamental competence for autonomous mobile robot navigation systems. The idea behind most of the current localisation systems operating in a known indoor environment is that the robot carries sensors to perceive the environment and match the obtained data with the expected data available in a map. The robot uses this operation to update its pose and correct the localisation error due to odometry slippage. In addition, sensor information can be used to simultaneously localise the robot and build the map of the environment along the robot's trajectory. The difficulty of the simultaneous localisation and map building (SLAM) problem lies in the fact that an accurate estimation of the robot trajectory is required to obtain a good map, and for reducing the unbounded growing odometry errors requires to associate sensor measurements with a precise map [14]. In order to increase the efficiency and robustness of the process, sensor data have to be transformed in a more compact form before attempting to compare them to the ones presented on a map or store them in a currently built map. In either case, the chosen map representation heavily determines the precision and reliability of the whole task [13]. Typical choices for the map representation include cell-based [6], topological [7], feature-based models [14] and sequential Monte Carlo methods [15]. In this paper, we adopt a feature-based approach for the map representation. This one allows the use of multiple models to describe the measurement process for different parts of the environment and it avoids the data smearing effect [14]. However, the success of this representation is conditioned on i) the existence of accurate sensors capable of discriminating between similar features and ii) the availability of fast and reliable algorithms capable of extracting features from a large set of noisy and uncertain data. Respect to the first question, sonar or laser range sensors or vision-

based systems can be employed. Sonar sensors suffer from frequent specular reflections and a significant spread of energy (beamwidth). Applying vision to feature extraction leads to increase CPU usage due to the complexity of the algorithms required. If we assume that the structural features commonly found in the environment are invariant to height (e.g. walls, corners, columns), a planar representation would be adequate for feature extraction. A laser range scanner is capable of collecting such high quality range data and it suffers from very small number of specular reflections. The angular uncertainty of the laser sensor is very small and, therefore, it can provide a very fine description of the surroundings to the robot. Finally, although from the perspective of cost, laser scanners are more expensive than sonar sensors, it can be appreciated that it is an affordable device for most robotic systems.

On the other hand, pattern recognition concepts and algorithms can be applied to extract features from sensor data. Thus, simple methods have been broadly used to support mobile robot operation using line or point features extracted from range images [16][5]. Although these methods are very fast, they have problems to deal with adverse phenomena such as false measurements on surface limits [4]. Besides, they do not consider sensor motion. More robust methods that take into account sensor motion have been also proposed [2][10]. These methods are based on more elaborate concepts, like the Hough Transform [2], the fuzzy clustering [4] or the Kalman Filter [13]. The main disadvantage of the majority of these methods is that they only look for one type of feature (e.g. line segment). Therefore, they are limited to find this feature in the measurement.

In this paper, the laser scan is analysed to detect rupture points and breakpoints [4] and three features of interest: line segments, corners and curve segments. Such items collect information about the environment as follows (see Fig. 1):

- Rupture points are scan measurements associated to discontinuities due to the absence of obstacles in the scanning direction.
- Breakpoints are scan discontinuities due to change of surface being scanned by the laser sensor.
- Line segments result from the scan of planar surfaces (e.g. walls).
- Corners are due to change of surface being scanned or to change in the orientation of the scanned surface. Corners are not associated to laser scan discontinuities.

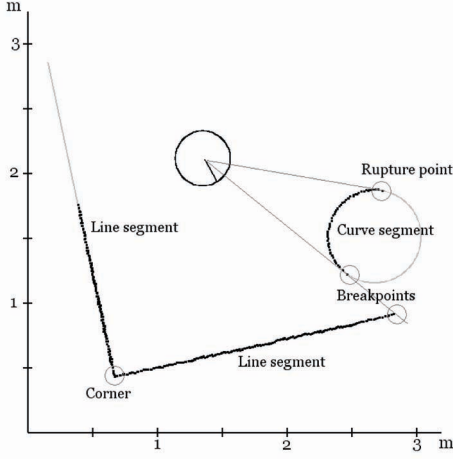


Fig. 1. Sensor information obtained from a single laser scan using a 180° SICK laser scanner.

- Curve segments result from the scan of curve surfaces (e.g. trees or cylindrical columns).

In what follows, we describe a geometrical feature detection framework for use with conventional 2D laser sensors. The framework is composed of three procedures: data acquisition and pre-processing, breakpoint detection and feature extraction. This scheme has been inspired from [5][4]. For data pre-processing and breakpoint detection, the motion correction algorithm proposed by Arras et al [2] and the adaptive algorithm proposed by Borges and Aldon [4] are respectively employed. The contribution of this paper is the feature extraction algorithm, which is based on adaptive curvature estimation. This algorithm uses the laser scan measurements between two consecutive breakpoints (or rupture points) like an open contour, and it permits to obtain line segments, corners and curve segments in a fast and robust way. The adaptive mechanism for curvature estimation avoids to employ a initially fixed threshold that may be problematic when different parts of the laser scan are analysed.

This paper has been organised as follows: Section 2 describes the characteristics of the laser sensor and the data pre-processing. Section 3 briefly presents the adaptive breakpoint detection method proposed by Borges and Aldon [4]. Section 4 describes the proposed algorithm for feature extraction based on curvature estimation. The adaptively estimated curvature function is introduced and its applications for line segment, corner and curve segment extraction is analysed. Section 5 presents experimental results and, finally, Section 6 summarises conclusions and future work.

## II. LASER SCAN DATA ACQUISITION AND PRE-PROCESSING

The information provided by laser sensors in a single scan is usually quite dense and has good angular precision. Range images provided by laser rangefinders are typically in the form  $\{(r, \phi)_l | l = 1 \dots N_R\}$ , on which  $(r, \phi)_l$  are the polar coordinates of the  $l$ -th range reading ( $r_l$  is the measured distance

of an obstacle to the sensor rotating axis at direction  $\phi_l$ ). The scan measurements are acquired by the laser rangefinder with a given angular resolution  $\Delta\phi = \phi_l - \phi_{l-1}$ . The distance  $r_l$  is perturbed by a systematic error,  $\epsilon_s$ , and a statistical error,  $\epsilon_r$ , usually assumed to follow a Gaussian distribution with zero mean and variance  $\sigma_r^2$ . Then, if  $r_m$  is the measured distance and  $r_t$  the true obstacle distance, it can be considered that they are related by

$$r_m - r_t = \epsilon_s(r_m) + \epsilon_r \quad (1)$$

Our laser rangefinder is a SICK Laser Measurement System (LMS) 200, and the experiments have been done with the LMS doing planar range scans with scanning angle of 180° operating at frequencies of about 60 Hz. In these conditions, the SICK LMS200 laser sensor exhibits a systematic error of  $\pm 15$  mm and a statistical error ( $\sigma_r$ ) of 5 mm. Taken several values of  $r_m$  for  $r_t \in [0.1, 8]$  m, the systematic error  $\epsilon_s(r_m)$  can be easily approximated by a sixth-order polynomial which fits the differences  $r_m - r_t$  in the least-squares sense [4]. This polynomial is used for compensating the systematic error according to the model (1). The residual noise after systematic error correction is compatible with the value  $\sigma_r = 0.005$  m provided by the laser rangefinder manufacturer.

When range images are taken with the robot in motion, they may be deformed given the scanning time. In such cases, a compensation algorithm based on estimates of the robot motion should be applied. In our system, the motion correction algorithm described in [2] is employed. Basically, this algorithm compensates for the vehicle displacement during a scan by transforming each range reading acquired at instant time  $t_l$  to the desired reference time  $t_0$ . Let  $\{(x, y)_l | l = 1 \dots N_R\}$  be the cartesian representation of the range images, where  $x_l = r_l \cos \phi_l$  and  $y_l = r_l \sin \phi_l$ , and  $p_l = (x_s, y_s, \theta_s)_l$  the sensor absolute position when the  $l$ -th range reading is acquired. At the  $l$ -th range reading acquisition, the local coordinate frame has been displaced  $p_d^l = p_l - p_0$  from the start of range reading acquisition. In order to recover the coordinates of the  $l$ -th range reading when the sensor is on  $p_0$ ,  $(x_l^0, y_l^0)$ , the sensor displacement is taken into account as

$$\begin{pmatrix} x_l^0 \\ y_l^0 \end{pmatrix} = \begin{pmatrix} \cos \theta_d^l & \sin \theta_d^l \\ -\sin \theta_d^l & \cos \theta_d^l \end{pmatrix} \cdot \begin{pmatrix} x_l + x_d^l \\ y_l + y_d^l \end{pmatrix} \quad (2)$$

Thus, it is not necessary to know the sensor absolute pose at each  $l^{th}$  point, but its relative displacement. In our experiments, it is assumed that odometry can provide a good estimation of this displacement. In fact, the operating frequency of the laser rangefinder is very high and the sensor displacement  $p_d^l$  is interpolated by a linear relation between  $p_d^0$  and  $p_d^{N_R}$ . These values can be derived from odometry.

Finally, at the same time that the systematic error and the motion are corrected, rupture points can be detected. A rupture point is defined as a discontinuity during the laser measurement. SICK LMS200 returns a special binary data to indicate this occurrence.

### III. BREAKPOINTS DETECTION

Segmentation is a process of aiming to classify each scan data into several groups, each of which possibly associates with different structures of the environment. The segmentation criterion is based on the distance between two consecutive points  $(r, \phi)_{l-1}$  and  $(r, \phi)_l$ . Range readings belong to the same segment while the distance between them is less than a given threshold. Isolated range readings are rejected. In order to determine the segment boundaries, we use the adaptive breakpoint detector developed by Borges and Aldon [4]. In this algorithm, two consecutive range readings belong to different segments if

$$|| (r, \phi)_l - (r, \phi)_{l-1} || > r_{l-1} \cdot \frac{\sin \Delta \phi}{\sin(\lambda - \Delta \phi)} + 3\sigma_r \quad (3)$$

where  $\Delta \phi$  is the laser angular resolution,  $\lambda$  is an auxiliary constant parameter and  $\sigma_r$  the residual variance. In our experiments, the parameter values are  $\sigma_r=0.005$  m and  $\lambda=10^\circ$  [4].

### IV. FEATURE EXTRACTION BASED ON ADAPTIVELY ESTIMATED CURVATURE FUNCTION

Curvature functions basically describe how much a curve bends at each point. The peaks of a curvature function correspond to the corners of the represented curve and their height depends on the angle at these corners. Flat segments whose average value is larger than zero are related to curve segments and those whose average value is equal to zero are related to straight line segments. Fig. 2a presents a curve yielding two corners (points 2 and 3) and a curve segment (from point 3 to 4). Peaks corresponding to 2 and 3 can be appreciated in its curvature function (Fig. 2b). It also shows that segment 3-4 has an average value larger than zero, but it is not flat due to noise. Nevertheless, peaks in that segment are too low to be considered corners of the curve. Finally, segments 1-2 and 2-3 present a curvature average value near to zero, as expected in line segments.

In order to calculate the curvature of a shape, Mokharian and Mackworth [9] employes a formula involving the first and second order directional derivatives of the shape coordinates, once the shape has been previously filtered with a one-dimensional Gaussian filter to remove noise. Agam and Dinstein [1] define the curvature at a given point as the difference between the slopes of the curve segments on the right and left side of the point, where slopes are taken from a look-up table. Liu and Srinath [8] calculate the curvature function by estimating the edge gradient at each shape point, which is equal to the arctangent of its Sobel difference in a 3x3 neighbourhood. Arrebola et al [3] define the curvature at a given point as the correlation of the forward and backward histograms in the  $k$ -vicinity of the point, where the resulting value is modified to include concavity and convexity information. It can be appreciated that most algorithms implicitly or explicitly filter the curve descriptor at a fixed cut frequency to remove noise and provide a more robust estimation of the curvature at each shape point. However, features appear at different natural

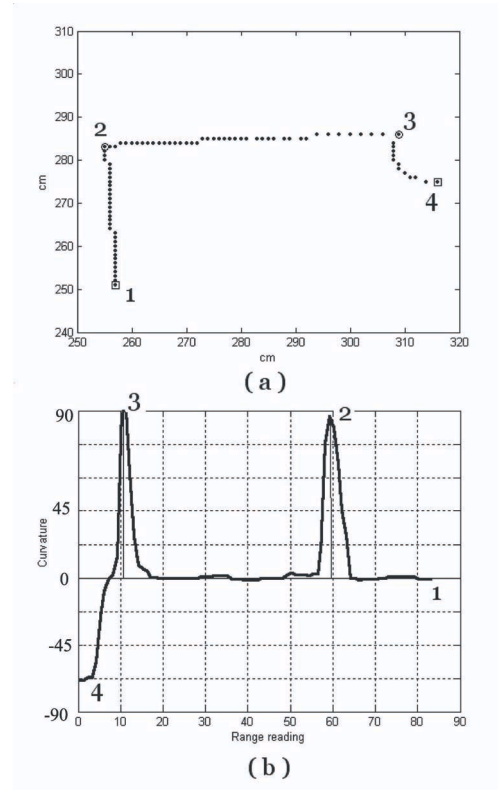


Fig. 2. a) Segment of a single laser scan ( $\square$ -breakpoints,  $\circ$ -detected corners); and b) curvature function associated to a).

scales and, since most methods filter the curve descriptor at a fixed cut frequency, only features unaffected by such a filtering process may be detected. Thus, algorithms described above basically consist of comparing segments of  $k$ -points at both sides of a given point to estimate its curvature. Therefore, the value of  $k$  determines the cut frequency of the curve filtering. In these methods, it is not easy to choose a correct  $k$  value: when  $k$  is small, the obtained curvature is very noisy and, when  $k$  is large, corners which are closer than  $k$  points are missed. To avoid this problem, some methods propose iterative feature detection for different cut frequencies, but they are slow and, in any case, they must choose the cut frequencies for each iteration.

In this work, we employ a curvature function that overcomes the aforementioned problems. Instead of choosing a constant  $k$  for the whole function,  $k$  is adaptively changed according to the distance between possible corners. Thus, the curve is filtered in an adaptive way depending on its local nature. In this case, noise is removed, but features are nevertheless detected despite their natural scale. The proposed method for adaptive curvature estimation in laser scan data is a modified version of [11] and, for each range reading  $i$  of a laser scan, it consists of the following steps:

- 1) Calculation of the maximum length of laser scan presenting no discontinuities on the right and left sides of the working range reading  $i$ :  $K_f[i]$  and  $K_b[i]$ , respectively.  $K_f[i]$  is the largest value that satisfies

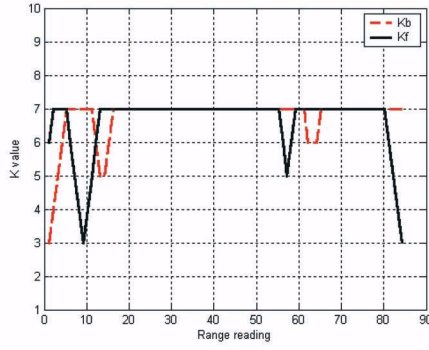


Fig. 3.  $K_f$  and  $K_b$  values associated to the range readings of the laser scan in Fig. 2a.

$$d(i, i + K_f[i]) > l(i, i + K_f[i]) - U_k \quad (4)$$

being  $U_k$  a constant value that depends on the noise level tolerated by the detector,  $(d(i, i + K_f[i]))$  is the Euclidean distance from range reading  $i$  to its  $K_f[i]$ -th neighbour and  $(l(i, i + K_f[i]))$  is the real length of the laser scan between both range readings. Both distances tend to be equal in absence of corners.

$K_b[i]$  is also set according to Eq. (4), but using  $i - K_b[i]$  instead of  $i + K_f[i]$ . The correct selection of the  $U_k$  value is very important. Thus, if the value of  $U_k$  is large,  $K_{f,b}[i]$  tends to be large and some corners may be missed and if it is small,  $K_{f,b}[i]$  is always very small and the resulting function is noisy. However, it is quite easy to fix a suitable  $U_k$  [11]. In our case, it has been proven that  $U_k=1.0$  works correctly in all our experiments. Fig. 3 presents an example of the  $K_f[i]$  and  $K_b[i]$  values associated to the range readings in Fig. 2a. It can be noted that the  $K_f[i]$  and  $K_b[i]$  values associate to range readings  $i$  located near to corner are reduced in order to accommodate them to the laser scan contour.

- 2) Calculation of the local vectors  $\vec{f}_i$  and  $\vec{b}_i$  associated to each range reading  $i$ . These vectors present the variation in the  $x$  and  $y$  axis between range readings  $i$  and  $i + K_f[i]$ , and between  $i$  and  $i - K_b[i]$ . If  $(x_i, y_i)$  are the coordinates of the range reading  $i$ , the local vectors associated to  $i$  are defined as

$$\begin{aligned} \vec{f}_i &= (x_{i+K_f[i]} - x_i, y_{i+K_f[i]} - y_i) = (f_{x_i}, f_{y_i}) \\ \vec{b}_i &= (x_{i-K_b[i]} - x_i, y_{i-K_b[i]} - y_i) = (b_{x_i}, b_{y_i}) \end{aligned} \quad (5)$$

- 3) Calculation of the angle associated to each range reading of the laser scan. According to the works of Rosenfeld and Johnston [12], the angle at range reading  $i$  can be estimated by using the equation:

$$\theta_i = \arccos \left( \frac{\vec{f}_i \cdot \vec{b}_i}{|\vec{f}_i| \cdot |\vec{b}_i|} \right) \quad (6)$$

- 4) Detection of line segments over  $|\theta_i|$ . Line segments result from the scan of planar surfaces. Therefore, they are those sets of consecutive range readings which: i) are under a minimum angle (in our experiments, this minimum curvature height,  $\theta_{min}$ , has been fixed at 0.05); and ii) have a size greater than a minimum length value ( $l_{min}=10$  range readings).
- 5) Detection of curve segments over  $|\theta_i|$ . Curve segments result from the scan of curve surfaces. Contrary to the curvature values associated to a line segment, it can be appreciated that the curvature function associated to a curve segment presents a consecutive set of local peaks, some of them could be wrongly considered as corners. To avoid this error, the algorithm associates a cornerity index to each set of consecutive range readings whose  $\theta_i$  values are over  $\theta_{min}$  or under  $-\theta_{min}$  and have a size greater than  $l_{min}$ . This cornerity index,  $ci$ , is defined as

$$ci = \frac{\frac{1}{i_e - i_b} \sum_{j=i_b}^{i_e} \theta_j}{\max_{i \in (i_b, i_e)} \{\theta_i\}} \quad (7)$$

where  $i_b$  and  $i_e$  are the range readings that bound the possible curve segment. These values are selected using a very low threshold in the curvature function. If  $ci$  is close to one, the mean curvature of the segment and its maximum value are similar, and the segment can be considered as a curve segment. If  $ci$  is low, the mean curvature of the segment is lower than its maximum value. Then, the segment cannot be considered as a curve segment. Therefore, curve segments are those sets of consecutive range readings which do not define a line segment and have a cornerity index greater than a given threshold  $U_c$  ( $U_c$  has been fixed at 0.5 in all experiments). Curve segments are characterised by its centre of curvature. In order to obtain it, we must previously obtain the radius of curvature  $\rho$ .

$$\rho = \frac{1}{\left( \frac{1}{i_e - i_b} \sum_{j=i_b}^{i_e} \theta_j \right) c} \quad (8)$$

where  $c$  is a constant that relates curvature values and centimetres. From  $\rho$ , we can obtain the centre of curvature associated,

$$\begin{aligned} x_c &= x_{ib} + \rho \cos(\theta \pm \pi/2) \\ y_c &= y_{ib} + \rho \sin(\theta \pm \pi/2) \end{aligned} \quad (9)$$

where  $\theta = \sum_{i=1}^{i_e} \theta_i$  is the accumulated angle at point  $(x_{ib}, y_{ib})$  and the sign of (9) is plus if the curve segment is concave and minor if it is convex.

- 6) Detection of corners over  $|\theta_i|$ . Although the corner value is a single curvature point, it is not defined in the curvature function as a Dirac delta function. Thus, the corner is always defined by a value associated to a local peak of the curvature function, and a region bounded by two range readings,  $i_b$  and  $i_e$ . Therefore, it can be characterised by a cornerity index,  $ci$ . Taken this into account, corners are those range readings which



do not belong to any line or curve segments and satisfy the following conditions: i) they are local peaks of the curvature function; ii) their  $|\theta_i|$  values are over the minimum angle required to be considered a corner instead of a spurious peak due to remaining noise ( $\theta_{min}$ ); iii) they are located between two segments which have been marked as line or curve segments, these two segments determine the region of the corner,  $(i_b, i_e)$ ; and iv) their cornerity indexes are lower than  $U_c$ .

The advantage of estimating the curvature in an adaptive way can be appreciated in Fig. 4. Fig. 4a shows a single laser scan between two breakpoints. The laser scan presents three corners, that have been marked with circles over the laser scan. It also consists of two line segments and a curve segment. Fig. 4b presents the curvature function associated to Fig. 4a obtained by the proposed algorithm. It can be noted that all features have been correctly detected. The limits that define each feature and the cornerity indexes of the curve segment and corners have been marked on the figure. Fig. 4c shows two curvature functions associated to Fig. 4a obtained by using two constant  $K$  values. It can be appreciated that when a low  $K$  value is used ( $K=5$ ), the curvature function is too noisy and false corner detections occur. On the contrary, if a high  $K$  value is used ( $K=15$ ), the laser scan is excessively filtered, and laser scan details might be lost.

## V. EXPERIMENTAL RESULTS

The feature extraction system has been implemented on two different mobile robots, an ActivMedia Pioneer2-AT that operates outdoors and a Nomadics Tech. Nomad200 that operates in an office-like indoor environment. Besides, during the experiments, people were walking around making the feature detection task even more challenging. To illustrate the accuracy of our method, two representative examples of its performance are shown in Fig. 5. Figs. 5a and 5b present two scan data collected in an indoor environment (our experiments in outdoors environment obtain a similar results). The laser scan range readings have been represented over the real layout. It can be appreciated that to acquire these two laser scans, the robot has been stopped, being the difference between laser scans due to there are two moving persons in front of it. Figs. 5c and 5d show the detected line segments, corners and curve segments associated to Figs. 5a and 5b, respectively. These indoor examples show the capability of the algorithm to correctly detect line and curve segments and corners and also the stability of these detections. The presence of the moving persons could be detected by analyzing the obtained results (segments 8 and 3 in Fig. 5d). Fig. 5e presents the curvature functions associated to the laser scan in Fig. 5b. The different curvature functions are bounded by breakpoints or rupture points. All features have been correctly detected, and it can be noted that several peaks presented in the curvature functions have been discarded as corners because they are not bounded by line or curve segments. Finally, the total time necessary to process the scan data is very reduced (less than 12 ms in a 400 MHz PC). Compared to other feature extraction

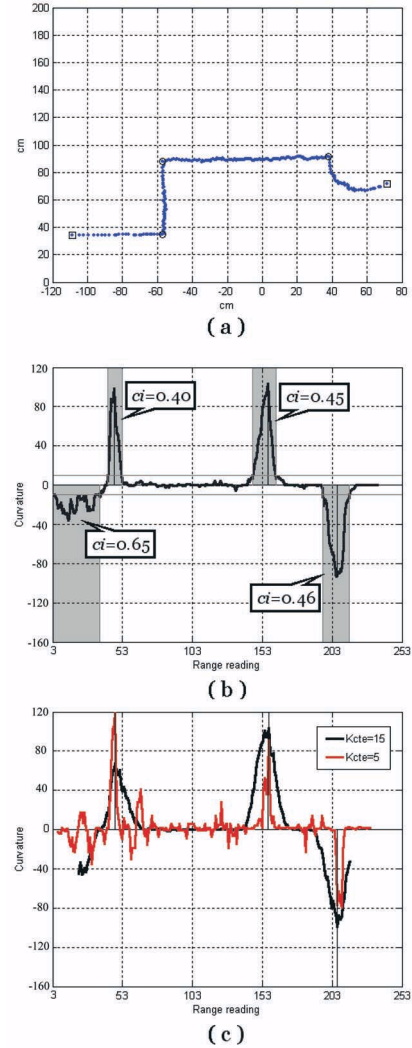


Fig. 4. a) Segment of a single laser scan ( $\square$ -breakpoints,  $\circ$ -detected corners); b) curvature function associated to a) obtained by using an adaptive  $K$  value; c) curvature functions associated to a) obtained by using a constant  $K$  value ( $K=5$  and  $K=15$ ).

algorithms, the proposed method permits to extract several features with very low computational requirements. In contrast to other algorithms that require iterative processing of the same laser scan [13], the described algorithm adaptively filters the laser scan depending on the natural scale of the contour range readings and determines easily the parameters of the features.

## VI. CONCLUSIONS AND FUTURE WORK

In this paper a new algorithm for feature extraction from laser scan data is presented. This algorithm can provide line segments, corners and curve segments to the mapping and localisation modules thus reducing the time required for a mobile robot to successfully localise itself. The main advantages of using an adaptive noise removal are that: i) features are detected at a wide range of scales for a constant set of detection parameters; and ii) estimated curvature is better defined. The accuracy and robustness of the proposed

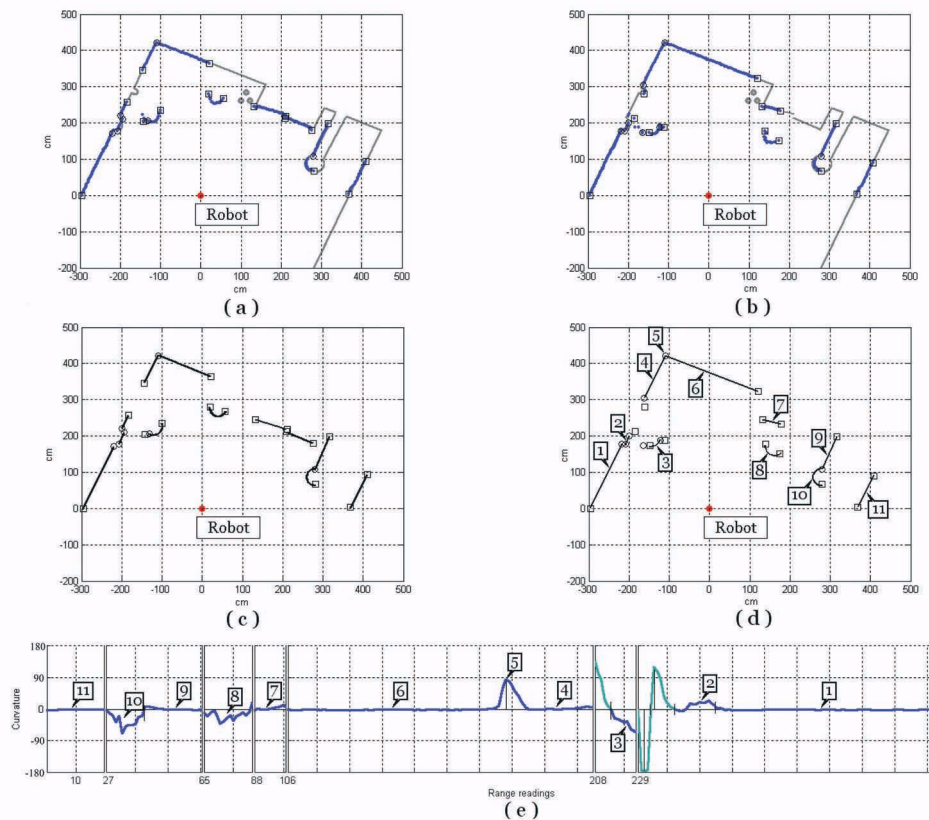


Fig. 5. a) Segmentation of the laser scan #1 ( $\square$ -breakpoints,  $\circ$ -detected corners); b) Segmentation of the laser scan #2 ( $\square$ -breakpoints,  $\circ$ -detected corners); c) line segments, corners and curve segments from a); d) line segments, corners and curve segments from b); and e) curvature functions associated to b).

method was demonstrated in a real world environment while meeting real-time requirements. Future work includes the development of an algorithm for robot localisation based on the extracted features and to test it in dynamics environments. This algorithm must be capable to differentiate static and dynamic parts of the environment and therefore, to represent only these static parts on a map. The union of the static map and the moving objects could provide a complete description of the environment.

#### ACKNOWLEDGMENT

This work has been partially granted by the Spanish Ministerio de Educación y Ciencia (MEC) and FEDER funds Project no. TIN2005-01349.

#### REFERENCES

- [1] G. Agam and I. Dinstein, "Geometric separation of partially overlapping nonrigid objects applied to automatic chromosome classification", *IEEE Trans. Pattern Analysis and Machine Intelligence* 11(19), pp. 1212-1222, 1997.
- [2] K. O. Arras, N. Tomatis, B. T. Jensen and R. Siegwart, "Multisensor on-the-fly localization: Precision and reliability for applications", *Robotics and Autonomous Systems* 34, pp. 131-143, 2001.
- [3] F. Arrebola, A. Bandera, P. Camacho and F. Sandoval, "Corner detection by local histograms of the contour chain code", *Electronics Letters* 33 (21), pp. 1769-1771, 1997.
- [4] G. A. Borges and M. Aldon, "Line extraction in 2D range images for mobile robotics", *Journal of Intelligent and Robotic Systems* 40, pp. 267-297, 2004.
- [5] J. A. Castellanos and J. D. Tardós, "Laser-based segmentation and localization for a mobile robot", in: M. Jamshidi, F. Pin and P. Dauchez (eds), *Robotics and Manufacturing: Recent Trends in Research and Applications*, Vol. 6, ASME Press, 1996.
- [6] A. Elfes, "Sonar-based real-world mapping and navigation", *IEEE Journal of Robotics and Automation* 3(3), pp. 249-265, 1987.
- [7] B. J. Kuipers, "The spatial semantic hierarchy", *Artificial Intelligence* 119, pp. 191-233, 2000.
- [8] H. Liu and D. Srinath, "Partial shape classification using contour matching in distance transformation", *IEEE Trans. Pattern Analysis and Machine Intelligence* 11(12), pp. 1072-1079, 1990.
- [9] F. Mokharian and A. Mackworth, "Scale-based description and recognition of planar curves and two-dimensional shapes", *IEEE Trans. Pattern Analysis and Machine Intelligence* 8, pp. 2-14, 1986.
- [10] N. E. Pears, "Feature extraction and tracking for scanning range sensors", *Robotics and Autonomous Systems* 33, pp. 43-58, 2000.
- [11] P. Reche, C. Urdiales, A. Bandera, C. Trazegnies and F. Sandoval, "Corner detection by means of contour local vectors", *Electronics Letters* 38 (14), pp. 699-701, 2002.
- [12] A. Rosenfeld and E. Johnston, "Angle detection on digital curves", *IEEE Trans. on Computers* 22, pp. 875-878, 1973.
- [13] S. Roumeliotis and G. A. Bekey, "SEGMENTS: A layered, dual-kalman filter algorithm for indoor feature extraction", *Proc. of the 2000 IEEE/RSJ Int. Conf. on Intelligent Robots and Systems*, pp. 454-461, 2000.
- [14] J. D. Tardós, J. Neira, P. M. Newman and J. J. Leonard, "Robust mapping and localization in indoor environments using sonar data", *Int. Journal of Robotics Research*, pp. 311-330, 2002.
- [15] S. Thrun, "An online mapping algorithm for teams of mobile robots", *Int. Journal of Robotics Research* 20(5), pp. 335-363, 2001.
- [16] L. Zhang and B. K. Ghosh, "Line segment based map building and localization using 2D laser rangefinder", *IEEE Int. Conf. on Robotics and Automation*, pp. 2538-2543, 2000.